Contrib Mineral Petrol (1992) 111:61–73

Contributions to Mineralogy and Petrology

Non-linear temperature dependence of liquid volumes in the system albite-anorthite-diopside

R. Knoche, D.B. Dingwell, and S.L. Webb

Bayerisches Geoinstitut, Universität Bayreuth, Postfach 10 12 51, W-8580 Bayreuth, Federal Republic of Germany

Received October 31, 1991 / Accepted January 22, 1992

Abstract. The temperature-dependent thermal expansivities of glasses and liquids in the ternary albite-anorthite-diopside have been determined using a combination of calorimetry, dilatometry and Pt and Ir double bob Archimedean densitometry. Supercooled liquid volumes and molar thermal expansivities were determined across the glass transition using a combination of scanning calorimetry and dilatometry, based upon the equivalence of relaxation of volume and enthalpy in the vicinity of the glass transition. Superliquidus volumes were determined using double Pt bob Archimedean densitometry at temperatures up to 1,650 °C and double Ir bob densitometry at 1,800 °C. Experimental access to liquid volumes near the glass transition temperatures (680–920 °C) and at superliquidus temperatures (1,400–1,800 °C) for these compositions results in the observation of a non-linear temperature dependence of molar volume, i.e., temperature-dependent thermal expansivities. The diopside composition exhibits the largest temperature dependence of thermal expansivity, decreasing by ~50% between 800 and 1,500 °C. Linear extrapolation of the high-temperature volume data of diopside to 810 °C would result in a 3% overestimation of the molar volume. The temperature dependence of the molar volume of anorthite is approximately linear. The thermal expansivities of the liquids in the albite-anorthite-diopside system appear to converge at high temperature. This study uses a combination of methods that allows interpolation rather than extrapolation of the extant melt-volume data into the petrologically meaningful (subliquidus) temperature range.

Introduction

A general equation of state for silicate melts is the ultimate goal of many experimentalists working on the mechanical and thermal properties of silicate liquids and glasses. Silicate melts are perhaps the key phase of matter in the chemical and physical evolution of the Earth and other terrestrial planets. Extensive investigations of the composition-dependence of silicate melt densities at superliquidus temperatures have yielded quantitative models for the prediction of melt volume at high temperature and 1 bar pressure (Bottinga and Weill 1970; Bottinga et al. 1983; Lange and Carmichael 1990). The temperature-dependence of melt volume, the expansivity, is much less well known (Bottinga et al. 1983). Thus, despite the abundant high-temperature volume data, the extrapolation of these data to magmatic temperatures is hampered by this lack of knowledge of thermal expansion for these liquids. The temperature range over which thermal expansion in silicate melts can be determined using traditional techniques is illustrated in Fig. 1. There is, in the example of Fig. 1, a ~700 °C gap between the glass transition temperature and the temperatures at which Archimedean densitometry measurements can be performed. Thermal-expansion data of sufficient precision would permit the extrapolation of these high-temperature determinations of volume from the experimentally accessible range (superliquidus) to the geologically relevant range, sometimes as much as 600 °C lower, where calcu-

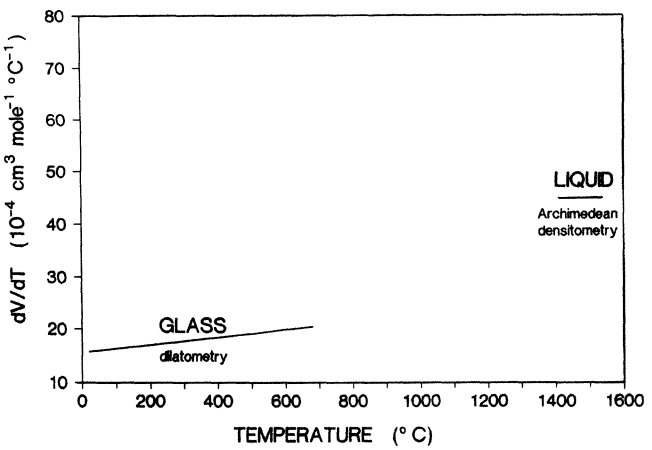

Fig. 1. Temperature range of molar thermal expansivity determinations by dilatometry and high temperature densitometry

lations of the physics of crystal-liquid fractionation, thermally and mechanically induced convection, and magma ascent are carried out. In order to test the predictive capabilities of volume models in temperature space, a set of volume and expansivity data obtained at magmatic temperatures is required. This implies, for most geological compositions, the determination of the properties of metastable liquids (i.e., above the glass transition and below the liquidus).

If the conditions of cooling are appropriate, many silicate melts avoid crystallization upon cooling to subsolidus temperatures and form glasses. The physical properties of these frozen liquids can be investigated, just above the glass transition, as true supercooled liquids (i.e., in metastable or local equilibrium) at temperatures and timescales that preclude significant crystallization or liquid-liquid unmixing. Use of these low-temperature metastable liquid data in combination with superliquidus liquid data for individual melt properties provides a wide temperature range over which the liquid behavior can be described.

The compositions used in this investigation lie in the ternary albite ($NaAlSi_3O_8$) – anorthite ($CaAl_2Si_2O_8$) – diopside ($CaMgSi_2O_6$). This system has been applied as a model for basalt petrogenesis (e.g., phase equilibria; Bowen 1915; Osborn and Tait 1952; Schairer and Yoder 1960; Kushiro 1973: thermochemistry; Weill et al. 1980; Navrotsky et al. 1980, 1989; viscosity; Scarfe et al. 1983; Scarfe and Cronin 1986; Tauber and Arndt 1987: ultrasonic wave velocities; Rivers and Carmichael 1987: shock wave equation of state; Rigden et al. 1988, 1989). The results of our determinations of thermal expansivity for the anorthite-diopside system have already been presented (Knoche et al. 1992a). Here we present data for the albite-anorthite and albite-diopside binaries as well as several compositions in the albite-anorthite-diopside ternary.

Methods

The glasses were obtained from M. Rosenhauer, Universität Göttingen. Their method of preparation is described by Tauber (1987). Microprobe analyses of these glasses are provided in Table 1. The theoretical compositions are also included in Table 1 for comparison. Viscosity data have been obtained on these samples over a wide temperature range by Tauber (1987) using the micropenetration method. A reconnaissance investigation of the glass transition temperature of these melts has been performed by Knoche (1990).

Calorimetry

The dilatometric and calorimetric investigations were performed on glass cylinders (25 mm long × 8 mm diameter) using methods described by Webb et al. (1992). The calorimetry was performed in continuous scanning mode using a Setaram® HTC instrument. The heat flow was recorded during heating runs of 5 °C/min on glasses that previously had been cooled at cooling rates of 1, 2, 5 and 10 °C/min. The calorimeter is calibrated regularly against a geometrically identical cylinder of sapphire, using the heat capacity data of Robie et al. (1979). The heat capacity data for the 5 °C min^{-1}/5 °C min^{-1} (cooling-rate/heating-rate) runs for all 24 compositions of the present study, together with the 5 compositions

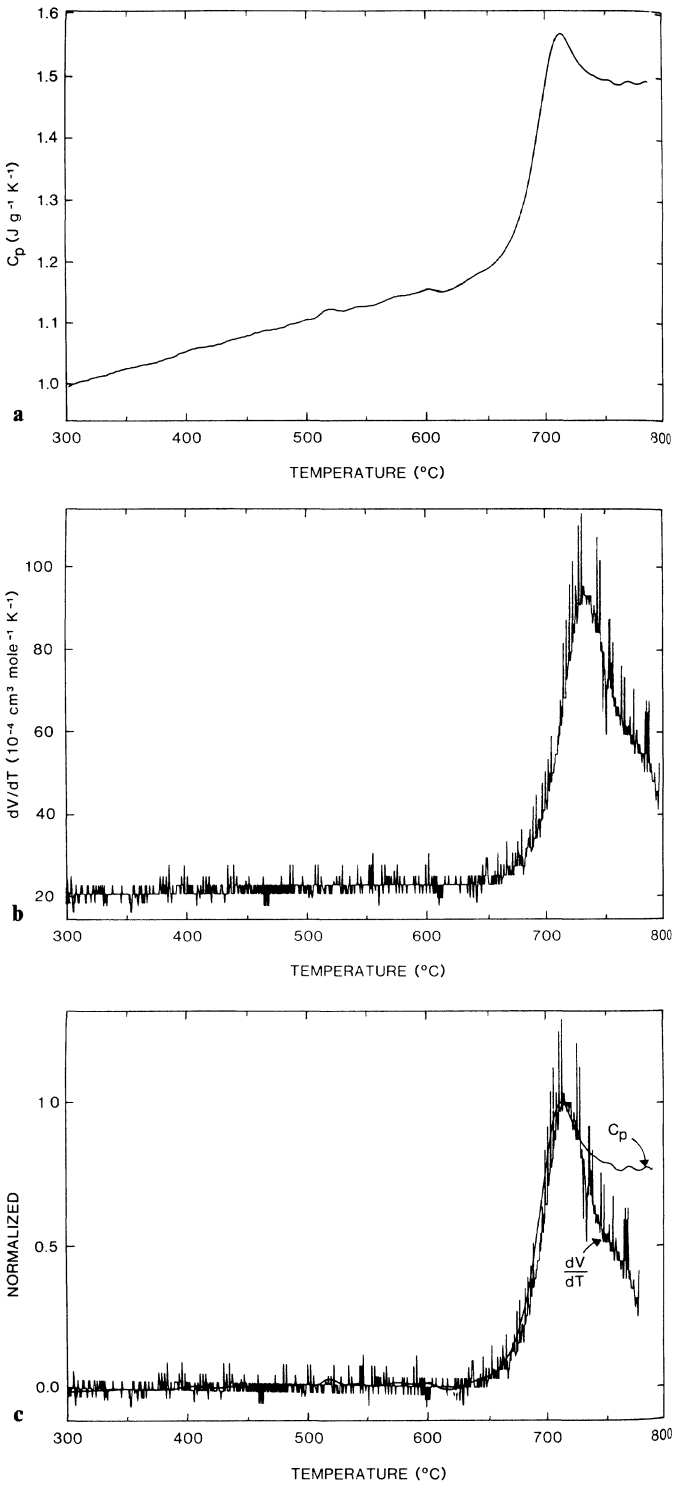

Fig. 2. a The calorimetry trace for $Ab_{42}An_{21}Di_{37}$ for a cooling rate of 5 °C min^{-1} and a heating rate of 5 °C min^{-1}. **b** The dilatometry trace for $Ab_{42}An_{21}Di_{37}$ for a cooling rate of 5 °C min^{-1} and a heating rate of 5 °C min^{-1}. **c** The method of normalization of the dilatometry and calorimetry traces for $Ab_{42}An_{21}Di_{37}$

of Knoche et al. (1992a), are presented in Table 2. The heat capacities are estimated to have a precision of ±2.5% at 1σ, based on the 4 runs performed for each sample. The measured heat capacities for the albite, anorthite and diopside glasses are within error of those determined by Stebbins et al. (1982, 1983) and Richet and Bottinga (1984a, b). A typical calorimetric trace, that obtained for $Ab_{42}An_{21}Di_{37}$ (5 °C min^{-1}/5 °C min^{-1}) is illustrated in Fig. 2a.

Table 1. Chemical composition of glasses (wt%)

		SiO_2	Al_2O_3	Na_2O	CaO	MgO	FeO	K_2O	Σ
Ab_{100}(B)		69.0	18.9	12.3	0.01	0.007	0.01	0.007	100.2
Ab_{100}(GM)		69.2	19.6	11.3	0.04	0.008	0.03	0.02	100.2
	Theor.	68.7	19.4	11.8					
$Ab_{95}An_{05}$(GM)		68.5	19.9	10.8	1.10	0.01	0.02	0.02	100.4
	Theor.	67.4	20.4	11.2	1.07				
$Ab_{80}An_{20}$(GM)		62.3	23.4	9.48	4.56	0.04	0.03	0.02	99.8
	Theor.	63.4	23.1	9.34	4.23				
$Ab_{50}An_{50}$(GM)		54.5	28.1	5.76	10.7	0.07	0.04	0.03	99.2
	Theor.	55.6	28.3	5.73	10.4				
$Ab_{30}An_{70}$(B)		50.2	30.9	3.37	14.7	0.08	0.01	0.007	99.3
	Theor.	50.5	31.7	3.40	14.4				
An_{100}(B)		43.0	35.1	0.01	20.5	0.10	0.02	0.005	98.7
An_{100}(GM)		42.9	35.1	0.18	20.7	0.08	0.07	0.02	99.1
	Theor.	43.2	36.7		20.2				
$An_{90}Di_{10}$(B)		44.6	32.4	0.04	20.5	1.43	0.02	0.009	99.0
	Theor.	44.2	33.7		20.6	1.48			
$An_{70}Di_{30}$(GM)		46.3	26.5	0.14	21.3	4.77	0.09	0.05	99.2
	Theor.	46.3	27.5		21.6	4.66			
$An_{50}Di_{50}$(GM)		47.3	19.9	0.12	25.0	6.88	0.08	0.02	99.3
	Theor.	48.6	20.6		22.7	8.15			
$An_{42}Di_{58}$(GM)		49.6	17.2	0.12	22.7	9.75	0.08	0.05	99.5
	Theor.	49.6	17.7		23.1	9.64			
$An_{20}Di_{80}$(GM)		52.3	8.70	0.08	24.3	14.1	0.09	0.06	99.6
	Theor.	52.5	8.91		24.5	14.1			
$An_{10}Di_{90}$(B)		55.6	4.47	0.09	24.7	14.6	0.01	0.002	99.5
	Theor.	54.0	4.58		25.2	16.3			
Di_{100}(B)		56.2	0.19	0.16	25.9	17.3	0.02	0.007	99.8
Di_{100}(GM)		55.0	0.22	0.05	25.6	18.5	0.09	0.06	99.5
	Theor.	55.5			25.9	18.6			
$Ab_{30}Di_{70}$(B)		60.1	6.54	4.08	17.3	11.6	0.007	0.01	99.6
	Theor.	60.0	6.64	4.04	17.1	12.3			
$Ab_{50}Di_{50}$(GM)		62.6	10.5	6.49	11.5	8.42	0.05	0.03	99.6
	Theor.	62.8	10.7	6.47	11.7	8.42			
$Ab_{70}Di_{30}$(B)		65.9	13.9	8.65	6.90	4.62	0.02	0.008	100.0
	Theor.	65.3	14.4	8.73	6.77	4.87			
$Ab_{80}Di_{20}$(GM)		66.5	16.0	9.77	4.44	3.24	0.03	0.02	100.0
	Theor.	66.5	16.1	9.80	4.43	3.18			
$Ab_{91}Di_{09}$(GM)		68.2	17.8	10.7	1.91	1.46	0.04	0.02	100.1
	Theor.	67.7	18.0	10.9	1.96	1.41			
$Ab_{95}Di_{05}$(GM)		67.8	18.5	11.6	1.13	0.81	0.03	0.03	99.9
	Theor.	68.2	18.6	11.3	1.08	0.78			
$Ab_{82.1}An_{03.7}Di_{14.2}$(N)		66.3	17.5	9.79	3.93	2.05	0.01	0.02	99.6
	Theor.	66.1	17.8	9.93	3.92	2.23			
$Ab_{69.8}An_{09.1}Di_{21.1}$(N)		63.5	17.1	8.22	6.75	3.34	0.01	0.009	99.0
	Theor.	63.8	17.7	8.51	6.67	3.35			
$Ab_{69.8}An_{09.1}Di_{21.1}$+As(N)		63.7	17.2	8.02	6.66	3.31	0.01	0.009	98.8
	Theor.	63.8	17.7	8.51	6.67	3.35			
$Ab_{55.6}An_{15.4}Di_{29.0}$(N)		60.4	16.8	6.81	9.93	4.53	0.01	0.01	98.6
	Theor.	61.1	17.5	6.85	9.90	4.65			
$Ab_{42.0}An_{21.1}Di_{36.8}$(N)		58.0	16.7	5.15	13.2	5.87	0.01	0.004	98.9
	Theor.	58.5	17.3	5.24	13.1	5.97			
$Ab_{28.1}An_{26.5}Di_{45.4}$(N)		55.3	16.2	3.54	16.5	7.29	0.01	0.008	98.9
	Theor.	55.8	16.8	3.54	16.4	7.45			
$Ab_{15.5}An_{31.7}Di_{52.8}$(N)		52.8	16.0	1.98	19.5	8.54	0.01	0.007	98.9
	Theor.	53.3	16.5	1.98	19.5	8.75			

Analysis by electron microprobe, Bayerisches Geoinstitut, operating conditions 15 kV accelerating voltage, 15 nA current on brass, 20 s count times using a 10 μm defocussed beam, standards wollastonite (Ca), diopside (Mg), albite (Si, Na), orthoclase (K), Fe_2O_3 (Fe), spinel (Al)

Theor. stoichiometric compositions.
B, N research grade chemicals
GM technical grade chemicals

Table 2a. Measured c_p ($Jg^{-1}\,°C^{-1}$) data for glasses and liquids. Cooling rate 5 °C min^{-1}; heating rate 5 °C min^{-1}
System Ab-An

T (°C)	Ab_{100}(B)	Ab_{100}(GM)	$Ab_{95}An_{05}$	$Ab_{80}An_{20}$	$Ab_{50}An_{50}$	$Ab_{30}An_{70}$
300	0.9977	1.0754	1.0581	0.9988	1.1149	
310	1.0021	1.0819	1.0646	1.0039	1.1253	
320	1.0100	1.0901	1.0718	1.0112	1.1361	
330	1.0194	1.0992	1.0785	1.0183	1.1495	
340	1.0181	1.0981	1.0767	1.0160	1.1575	
350	1.0191	1.1017	1.0790	1.0201	1.1664	1.0776
360	1.0237	1.1048	1.0852	1.0252	1.1738	1.0833
370	1.0327	1.1097	1.0927	1.0322	1.1804	1.0857
380	1.0389	1.1164	1.1005	1.0402	1.1833	1.0896
390	1.0456	1.1248	1.1050	1.0445	1.1965	1.0972
400	1.0552	1.1309	1.1124	1.0526	1.2053	1.1108
410	1.0586	1.1325	1.1186	1.0616	1.2074	1.1104
420	1.0611	1.1358	1.1214	1.0652	1.2161	1.1154
430	1.0662	1.1386	1.1235	1.0667	1.2242	1.1240
440	1.0722	1.1440	1.1311	1.0700	1.2313	1.1278
450	1.0766	1.1528	1.1380	1.0770	1.2390	1.1342
460	1.0796	1.1565	1.1397	1.0796	1.2452	1.1425
470	1.0827	1.1649	1.1388	1.0813	1.2553	1.1489
480	1.0866	1.1736	1.1434	1.0877	1.2622	1.1552
490	1.0918	1.1712	1.1495	1.0932	1.2706	1.1631
500	1.0974	1.1716	1.1524	1.0945	1.2782	1.1666
510	1.1020	1.1767	1.1589	1.1031	1.2827	1.1718
520	1.1013	1.1817	1.1607	1.1057	1.2916	1.1830
530	1.1088	1.1894	1.1666	1.1154	1.3056	1.1925
540	1.1196	1.2021	1.1803	1.1164	1.3134	1.2000
550	1.1220	1.2086	1.1847	1.1165	1.3186	1.2048
560	1.1206	1.2048	1.1813	1.1150	1.3291	1.2156
570	1.1236	1.2101	1.1814	1.1249	1.3370	1.2206
580	1.1288	1.2178	1.1902	1.1338	1.3434	1.2278
590	1.1317	1.2214	1.1940	1.1372	1.3501	1.2370
600	1.1401	1.2306	1.1993	1.1409	1.3570	1.2439
610	1.1465	1.2389	1.2047	1.1514	1.3644	1.2499
620	1.1482	1.2364	1.2028	1.1478	1.3711	1.2506
630	1.1487	1.2464	1.1979	1.1383	1.3792	1.2586
640	1.1577	1.2611	1.2023	1.1397	1.3845	1.2614
650	1.1759	1.2669	1.2139	1.1466	1.3918	1.2655
660	1.1928	1.2623	1.2205	1.1502	1.3959	1.2751
670	1.2206	1.2675	1.2222	1.1513	1.4043	1.2796
680	1.2516	1.2607	1.2201	1.1482	1.4114	1.2834
690	1.2845	1.2706	1.2203	1.1469	1.4182	1.2942
700	1.3134	1.2799	1.2229	1.1494	1.4258	1.3113
710	1.3245	1.2914	1.2190	1.1617	1.4313	1.2977
720	1.3157	1.3087	1.2227	1.1719	1.4384	1.2981
730	1.3009	1.3202	1.2305	1.1713	1.4484	1.3067
740	1.2928	1.3309	1.2420	1.1783	1.4605	1.3167
750	1.2845	1.3467	1.2517	1.1946	1.4763	1.3253
760	1.2762	1.3762	1.2741	1.2308	1.5054	1.3404
770	1.2707	1.4354	1.3027	1.2833	1.5487	1.3568
780	1.2685	1.4595	1.3362	1.3428	1.6073	1.3845
790	1.2650	1.4771	1.3687	1.3766	1.7038	1.4373
800	1.2673	1.4966	1.3957	1.3641	1.8028	1.5137
810		1.5071	1.3987	1.3356	1.8398	1.6195
820		1.4816	1.3670	1.3104	1.8090	1.7296
830		1.4611	1.3181	1.2925	1.7780	1.7562
840		1.4566	1.3063	1.2525	1.7695	1.7156
850		1.4539	1.3123	1.2614	1.7698	1.6910
860		1.4319	1.2979	1.2499	1.7706	1.6829
870		1.4270	1.2986	1.2444	1.7752	1.6825
880		1.4242	1.3101	1.2522	1.7790	1.6731
890						1.6673
900						1.6661
910						
920						
930						
940						
950						
Peak temperature	705 °C	803 °C	801 °C	790 °C	805 °C	824 °C

Table 2b. Measured c_p (J g^{-1} $°C^{-1}$) data for glasses and liquids. Cooling rate 5 °C min^{-1}; heating rate 5 °C min^{-1}

System An—Di

T (°C)	An_{100}(B)	An_{100}(GM)	$An_{90}Di_{10}$	$An_{70}Di_{30}$	$An_{50}Di_{50}$	$An_{42}Di_{58}$	$An_{20}Di_{80}$	$An_{10}Di_{90}$	Di_{100}(B)	Di_{100}(GM)
300				1.0279	1.0117	0.9727	0.9971		1.0043	1.0008
310				1.0338	1.0147	0.9795	1.0033		1.0105	1.0048
320				1.0378	1.0180	0.9876	1.0054		1.0148	1.0121
330				1.0380	1.0216	0.9921	1.0098		1.0208	1.0127
340				1.0487	1.0273	0.9960	1.0163		1.0230	1.0140
350			0.9477	1.0608	1.0351	0.9978	1.0195	1.0241	1.0251	1.0120
360			0.9485	1.0651	1.0383	1.0084	1.0270	1.0332	1.0321	1.0091
370			0.9502	1.0696	1.0437	1.0167	1.0328	1.0422	1.0374	1.0169
380			0.9546	1.0750	1.0515	1.0229	1.0365	1.0449	1.0403	1.0240
390			0.9609	1.0813	1.0559	1.0244	1.0432	1.0472	1.0402	1.0263
400	1.0243	1.0304	0.9687	1.0862	1.0609	1.0250	1.0479	1.0569	1.0460	1.0333
410	1.0225	1.0339	0.9686	1.0885	1.0658	1.0280	1.0486	1.0602	1.0559	1.0324
420	1.0249	1.0410	0.9752	1.0902	1.0673	1.0304	1.0487	1.0644	1.0716	1.0331
430	1.0293	1.0456	0.9820	1.0931	1.0705	1.0353	1.0536	1.0733	1.0800	1.0413
440	1.0310	1.0508	0.9879	1.1012	1.0757	1.0389	1.0607	1.0769	1.0604	1.0436
450	1.0350	1.0539	0.9915	1.1058	1.0830	1.0440	1.0617	1.0841	1.0309	1.0457
460	1.0377	1.0560	0.9937	1.1063	1.0842	1.0544	1.0674	1.0972	1.0457	1.0504
470	1.0445	1.0591	1.0030	1.1135	1.0897	1.0600	1.0702	1.0992	1.0745	1.0535
480	1.0390	1.0638	1.0022	1.1178	1.0944	1.0672	1.0749	1.1030	1.0947	1.0493
490	1.0437	1.0702	1.0049	1.1209	1.0928	1.0718	1.0821	1.1036	1.1048	1.0563
500	1.0498	1.0774	1.0150	1.1253	1.0970	1.0746	1.0878	1.1020	1.1170	1.0611
510	1.0633	1.0871	1.0196	1.1269	1.0969	1.0801	1.0951	1.1159	1.1263	1.0678
520	1.0617	1.0844	1.0248	1.1274	1.1038	1.0783	1.0953	1.1240	1.1409	1.0741
530	1.0538	1.0859	1.0238	1.1390	1.1111	1.0805	1.0988	1.1259	1.1469	1.0715
540	1.0535	1.0888	1.0300	1.1427	1.1102	1.0878	1.1055	1.1367	1.1460	1.0749
550	1.0662	1.0945	1.0385	1.1476	1.1153	1.0932	1.1093	1.1452	1.1601	1.0836
560	1.0759	1.0964	1.0391	1.1512	1.1214	1.1036	1.1195	1.1528	1.1619	1.0914
570	1.0769	1.1002	1.0468	1.1562	1.1241	1.1067	1.1235	1.1645	1.1681	1.0953
580	1.0919	1.1050	1.0483	1.1635	1.1312	1.1093	1.1290	1.1737	1.1862	1.1091
590	1.0901	1.1082	1.0552	1.1679	1.1331	1.1176	1.1346	1.1799	1.1857	1.1084
600	1.0885	1.1140	1.0711	1.1740	1.1408	1.1185	1.1350	1.1732	1.1856	1.1130
610	1.0946	1.1234	1.0757	1.1758	1.1471	1.1258	1.1390	1.1852	1.1911	1.1162
620	1.1014	1.1258	1.0871	1.1778	1.1490	1.1350	1.1467	1.1949	1.2027	1.1172
630	1.1101	1.1258	1.0799	1.1818	1.1552	1.1422	1.1494	1.2044	1.2023	1.1252
640	1.1114	1.1293	1.0832	1.1874	1.1577	1.1524	1.1576	1.2103	1.1775	1.1267
650	1.1068	1.1312	1.0937	1.1934	1.1610	1.1505	1.1551	1.2097	1.1804	1.1243
660	1.1085	1.1357	1.1003	1.1958	1.1612	1.1551	1.1553	1.2217	1.1980	1.1293
670	1.1208	1.1393	1.1032	1.2007	1.1687	1.1689	1.1652	1.2410	1.2341	1.1325
680	1.1273	1.1417	1.1179	1.2029	1.1700	1.1767	1.1734	1.2557	1.2676	1.1515
690	1.1256	1.1444	1.1198	1.2213	1.1909	1.1899	1.1917	1.2795	1.2969	1.1681
700	1.1239	1.1494	1.1153	1.2254	1.1972	1.2118	1.2295	1.3324	1.3646	1.2046
710	1.1386	1.1537	1.1276	1.2307	1.2102	1.2379	1.2933	1.4180	1.4856	1.2748
720	1.1340	1.1581	1.1264	1.2328	1.2297	1.2874	1.4125	1.5485	1.6536	1.3941
730	1.1290	1.1617	1.1322	1.2412	1.2679	1.3691	1.5781	1.7184	1.7955	1.5771
740	1.1352	1.1663	1.1451	1.2603	1.3482	1.5164	1.6653	1.7623	1.7860	1.6580
750	1.1308	1.1703	1.1444	1.2889	1.4675	1.6515	1.6214	1.7110	1.7402	1.6017
760	1.1271	1.1706	1.1515	1.3473	1.6078	1.6568	1.5824	1.6855	1.7085	1.5675
770	1.1373	1.1761	1.1544	1.4491	1.6494	1.6078	1.5622	1.6776	1.6929	1.5537
780	1.1428	1.1856	1.1588	1.5768	1.6060	1.5853	1.5550	1.6656	1.6821	1.5404
790	1.1441	1.1924	1.1792	1.6727	1.5735	1.5696	1.5502	1.6636	1.6749	1.5289
800	1.1480	1.2073	1.2120	1.6637	1.5546	1.5636		1.6633	1.6782	1.5343
810	1.1716	1.2323	1.2602	1.6322	1.5476	1.5609				
820	1.1979	1.2614	1.3454	1.6058	1.5468					
830	1.2224	1.3107	1.4711	1.5981						
840	1.2880	1.4001	1.5984	1.5970						
850	1.3931	1.5334	1.6271	1.6022						
860	1.5135	1.6685	1.5779							
870	1.6108	1.6728	1.5494							
880	1.5905	1.6172	1.5352							
890	1.5457	1.5830	1.5267							
900	1.5235	1.5770	1.5231							
910	1.5155	1.5737								
920	1.5104	1.5684								
930	1.5068	1.5666								
940	1.5041									
950	1.5148									
Peak temperature	868 °C	863 °C	844 °C	792 °C	769 °C	752 °C	740 °C	734 °C	732 °C	736 °C

Table 2c. Measured c_p (J g^{-1} $°C^{-1}$) data for glasses and liquids. Cooling rate 5 °C min^{-1}; heating rate 5 °C min^{-1}
System Di – Ab

T (°C)	$Ab_{30}Di_{70}$	$Ab_{50}Di_{50}$	$Ab_{70}Di_{30}$	$Ab_{80}Di_{20}$	$Ab_{91}Di_{09}$	$AB_{95}Di_{05}$
300	1.0191		1.0082	0.9791	1.0325	1.0703
310	1.0289		1.0135	0.9870	1.0388	1.0773
320	1.0395		1.0208	0.9927	1.0472	1.0859
330	1.0456		1.0313	1.0015	1.0564	1.0972
340	1.0471		1.0287	1.0032	1.0547	1.0968
350	1.0505		1.0317	1.0086	1.0561	1.1000
360	1.0611		1.0385	1.0160	1.0647	1.1073
370	1.0709		1.0462	1.0243	1.0722	1.1161
380	1.0827		1.0552	1.0328	1.0787	1.1252
390	1.0830		1.0624	1.0391	1.0851	1.1337
400	1.0845		1.0742	1.0542	1.0954	1,1437
410	1.0889		1.0790	1.0573	1.1024	1.1502
420	1.1027		1.0810	1.0564	1.1054	1.1530
430	1.0791		1.0842	1.0611	1.1106	1.1564
440	1.0512		1.0911	1.0681	1.1166	1.1703
450	1.0886		1.0983	1.0794	1.1235	1.1767
460	1.1321	1.0704	1.1042	1.0827	1.1287	1.1755
470	1.1633	1.0722	1.1078	1.0869	1.1344	1.1789
480	1.1753	1.0798	1.1163	1.0933	1.1415	1.1846
490	1.1775	1.0877	1.1235	1.1053	1.1461	1.1932
500	1.1820	1.0901	1.1270	1.1080	1.1502	1.2014
510	1.1877	1.0947	1.1373	1.1137	1.1591	1.2093
520	1.1946	1.0863	1.1411	1.1165	1.1617	1.2135
530	1.2007	1.0957	1.1449	1.1264	1.1700	1.2221
540	1.2153	1.1190	1.1555	1.1372	1.1816	1.2330
550	1.2176	1.1243	1.1732	1.1405	1.1877	1.2379
560	1.2126	1.1274	1.1758	1.1395	1.1901	1.2393
570	1.2139	1.1355	1.1663	1.1466	1.1948	1.2446
580	1.2193	1.1328	1.1659	1.1661	1.2016	1.2529
590	1.2155	1.1307	1.1766	1.1656	1.2052	1.2563
600	1.2338	1.1404	1.1905	1.1648	1.2128	1.2604
610	1.2769	1.1503	1.1996	1.1781	1.2241	1.2685
620	1.3068	1.1553	1.2108	1.1840	1.2287	1.2727
630	1.3217	1.1687	1.2245	1.1891	1.2310	1.2724
640	1.3619	1.2088	1.2561	1.2150	1.2430	1.2837
650	1.3655	1.2722	1.3141	1.2526	1.2621	1.2978
660	1.3969	1.3585	1.3900	1.3002	1.2837	1.3029
670	1.5195	1.4793	1.4789	1.3661	1.3203	1.3121
680	1.6895	1.5693	1.5409	1.4363	1.3422	1.3264
690	1.7524	1.5653	1.5425	1.4747	1.3771	1.3440
700	1.6945	1.5312	1.5186	1.4648	1.4188	1.3731
710	1.6361	1.5118	1.5030	1.4442	1.4546	1.4091
720	1.6255	1.5044	1.4990	1.4335	1.4781	1.4521
730	1.6360	1.4962	1.4947	1.4312	1.4739	1.4872
740	1.6555	1.4926	1.4907	1.4300	1.4605	1.5108
750	1.6597	1.4889	1.4887	1.4248	1.4517	1.5034
760	1.6542	1.4913	1.4910	1.4226	1.4453	1.4897
770			1.4901	1.4202	1.4425	1.4859
780				1.4238	1.4560	1.4879
790					1.4608	1.4817
800					1.4543	1.4769
810						1.4801
820						
830						
840						
850						
860						
870						
880						
890						
900						
910						
920						
930						
940						
950						
Peak temperature	686 °C	680 °C	680 °C	687 °C	718 °C	738 °C

Table 2d. Measured c_p (J g^{-1} $°C^{-1}$) data for glasses and liquids. Cooling rate 5 °C min^{-1}; heating rate 5 °C min^{-1}
System Ab–An–Di: ternary samples

T (°C)	$Ab_{82}An_{04}$ Di_{14}	$Ab_{70}An_{09}$ Di_{21}	$Ab_{70}An_{09}$ Di_{21}(+As)	$Ab_{56}An_{15}$ Di_{29}	$Ab_{42}An_{21}$ Di_{37}	$Ab_{28}An_{27}$ Di_{45}	$Ab_{15}An_{32}$ Di_{53}
300	1.0187	0.9911	1.0402	1.0293	0.9969	0.9986	0.9636
310	1.0263	0.9981	1.0465	1.0345	1.0059	1.0046	0.9657
320	1.0302	1.0010	1.0506	1.0375	1.0116	1.0105	0.9746
330	1.0414	1.0137	1.0648	1.0488	1.0159	1.0128	0.9791
340	1.0507	1.0197	1.0723	1.0561	1.0226	1.0145	0.9802
350	1.0552	1.0245	1.0776	1.0588	1.0278	1.0150	0.9818
360	1.0555	1.0239	1.0746	1.0618	1.0319	1.0225	0.9862
370	1.0578	1.0284	1.0791	1.0678	1.0356	1.0248	0.9895
380	1.0696	1.0346	1.0910	1.0744	1.0411	1.0274	0.9912
390	1.0758	1.0398	1.0966	1.0803	1.0472	1.0347	0.9979
400	1.0733	1.0440	1.0974	1.0817	1.0555	1.0417	1.0040
410	1.0801	1.0499	1.1034	1.0882	1.0613	1.0413	1.0032
420	1.0891	1.0561	1.1096	1.0972	1.0637	1.0472	1.0079
430	1.0940	1.0627	1.1144	1.1029	1.0685	1.0579	1.0163
440	1.0963	1.0664	1.1156	1.1086	1.0748	1.0576	1.0172
450	1.1034	1.0715	1.1231	1.1133	1.0801	1.0582	1.0194
460	1.1103	1.0805	1.1319	1.1159	1.0855	1.0656	1.0273
470	1.1147	1.0837	1.1337	1.1202	1.0895	1.0690	1.0282
480	1.1212	1.0849	1.1400	1.1259	1.0935	1.0725	1.0295
490	1.1255	1.0917	1.1452	1.1287	1.1001	1.0758	1.0343
500	1.1300	1.0997	1.1513	1.1359	1.1065	1.0817	1.0394
510	1.1355	1.1062	1.1583	1.1452	1.1129	1.0851	1.0440
520	1.1479	1.1129	1.1704	1.1494	1.1236	1.0914	1.0507
530	1.1507	1.1169	1.1719	1.1519	1.1200	1.0940	1.0536
540	1.1494	1.1176	1.1700	1.1526	1.1264	1.0967	1.0583
550	1.1589	1.1217	1.1765	1.1601	1.1278	1.1009	1.0598
560	1.1625	1.1259	1.1805	1.1625	1.1325	1.1088	1.0629
570	1.1704	1.1363	1.1892	1.1708	1.1406	1.1119	1.0695
580	1.1721	1.1543	1.1908	1.1755	1.1452	1.1105	1.0708
590	1.1743	1.1558	1.1954	1.1783	1.1487	1.1162	1.0724
600	1.1776	1.1388	1.1958	1.1814	1.1557	1.1223	1.0770
610	1.1798	1.1423	1.1983	1.1819	1.1416	1.1100	1.0639
620	1.1836	1.1441	1.1959	1.1829	1.1487	1.1139	1.0676
630	1.1907	1.1466	1.2003	1.1870	1.1647	1.1264	1.0782
640	1.2153	1.1710	1.2230	1.2147	1.1774	1.1350	1.0945
650	1.2362	1.1879	1.2337	1.2329	1.1879	1.1380	1.0883
660	1.2493	1.1947	1.2371	1.2415	1.2047	1.1465	1.0975
670	1.2662	1.2229	1.2624	1.2809	1.2342	1.1687	1.1079
680	1.3266	1.2716	1.3033	1.3531	1.2857	1.2122	1.1282
690	1.3945	1.3470	1.3713	1.4560	1.3712	1.2563	1.1515
700	1.4357	1.4289	1.4474	1.5291	1.4864	1.3602	1.2177
710	1.4489	1.4658	1.5031	1.5261	1.5636	1.4936	1.3371
720	1.4350	1.4485	1.4987	1.4943	1.5497	1.5577	1.4752
730	1.4184	1.4223	1.4707	1.4745	1.5169	1.5328	1.5280
740	1.4033	1.4035	1.4415	1.4552	1.5015	1.5051	1.4894
750	1.4094	1.3993	1.4400	1.4507	1.4943	1.4827	1.4561
760	1.3965	1.3846	1.4225	1.4324	1.4864	1.4571	1.4347
770	1.3943	1.3786	1.4213	1.4286	1.4917	1.4609	1.4257
780	1.3974	1.3846	1.4233	1.4323	1.4897	1.4593	1.4211
790	1.3938	1.3783	1.4217		1.4904	1.4765	1.4175
800							
810							
820							
830							
840							
850							
860							
870							
880							
890							
900							
910							
920							
930							
940							
950							
Peak temperature	701 °C	706 °C	710 °C	700 °C	709 °C	716 °C	725 °C

Dilatometry

The dilatometry was performed using a Netzsch® TMA 402 quartz-rod dilatometer. The samples, their thermal history and the scanning rates were those used in the calorimetry measurements. This instrument has been calibrated against sapphire (NBS sheet 732) and the molar expansivities have an accuracy of $\pm 3\%$ at 1σ, calculated from the errors in the measurements of the thermal expansivity of the standard and the sample. The molar volumes, calculated from the room-temperature density data combined with the dilatometric data for the glasses, are presented in Table 3. The dilatometry trace for $Ab_{42}An_{21}Di_{37}$ (5 °C min^{-1}/5 °C min^{-1}) is illustrated in Fig. 2b.

Table 3. Molar volume (cm^3) of glasses as a function of temperature and density (g cm^{-3}) at room temperature (21.3 °C). V(cm^3 mole^{-1})$=a+b\times10^{-4}\,T+c\times10^{-7}\,T^2$ with T=temperature in °C

	a	b	c	T	Density
Ab_{100}(B)	109.26	25.83	0.08	20–610	2.399
Ab_{100}(GM)	110.11	21.04	3.04	20–690	2.381
$Ab_{95}An_{05}$	108.87	22.02	2.18	20–700	2.415
$Ab_{80}An_{20}$	108.59	20.90	4.03	20–700	2.443
$Ab_{50}An_{50}$	105.34	18.51	2.12	20–710	2.564
$Ab_{30}An_{70}$	104.37	16.38	2.64	20–730	2.619
An_{100}(B)	102.87	15.00	2.94	20–780	2.704
An_{100}(GM)	102.47	15.18	4.62	20–770	2.714
$An_{90}Di_{10}$	100.46	15.22	3.05	20–750	2.707
$An_{70}Di_{30}$	94.94	14.72	4.50	20–710	2.735
$An_{50}Di_{50}$	88.83	16.53	3.57	20–680	2.784
$An_{42}Di_{58}$	87.21	16.09	3.88	20–670	2.779
$An_{20}Di_{80}$	81.01	15.54	5.07	20–660	2.824
$An_{10}Di_{90}$	79.00	15.13	5.97	20–660	2.818
Di_{100}(B)	75.93	14.25	8.75	20–660	2.851
Di_{100}(GM)	75.61	16.89	5.03	20–670	2.863
$Ab_{30}Di_{70}$	85.09	15.79	8.10	20–620	2.705
$Ab_{50}Di_{50}$	91.96	18.36	5.63	20–610	2.602
$Ab_{70}Di_{30}$	99.01	18.87	5.79	20–610	2.509
$Ab_{80}Di_{20}$	102.11	20.72	4.90	20–600	2.477
$Ab_{91}Di_{09}$	106.35	22.76	3.14	20–600	2.426
$Ab_{95}Di_{05}$	107.50	25.28	0.67	20–620	2.417
$Ab_{82}An_{04}Di_{14}$	104.15	22.06	2.31	20–610	2.460
$Ab_{70}An_{09}Di_{21}$	101.34	19.78	3.47	20–620	2.506
$Ab_{70}An_{09}Di_{21}$ (+As)	101.43	20.36	2.58	20–620	2.504
$Ab_{56}An_{15}Di_{29}$	98.04	19.48	3.39	20–610	2.564
$Ab_{42}An_{21}Di_{37}$	94.94	17.12	4.95	20–620	2.617
$Ab_{28}An_{27}Di_{45}$	91.74	15.47	6.15	20–630	2.677
$Ab_{15}An_{32}Di_{53}$	88.78	17.46	3.59	20–650	2.738

Cooling/heating rate: 5/5 (°C min^{-1}); density is $\pm 0.2\%$ at 1σ

Pt and Ir double bob densitometry

The high-temperature Pt double bob Archimedean densitometry was performed using the apparatus described by Dingwell et al. (1988). The determination of liquid albite density was performed at 1,800 °C using iridium crucible and bobs and a ZrO_2-based very high temperature furnace. The method is described by Dingwell (1991). High-temperature densities obtained using these methods have a precision of $\pm 0.2\%$ and $\pm 0.3\%$, respectively for the Pt and Ir-based systems and reproduce the best value for molten NaCl within this precision at lower temperatures (Janz 1980). For the case of albite melt, investigated at 1,800 °C, the melt composition was reanalyzed after Ir double bob determinations. The analyses of the melt before and after these measurements indicated a Na loss of $\sim 0.5\%$. The final composition is stoichiometric albite. Room-temperature densities of the glass cylinders were measured using Archimedean buoyancy in toluene and have a precision of $\pm 0.2\%$. The measured glass and liquid densities, together with the calculated molar volumes are presented in Table 4.

Theory

The derivation of liquid expansivity and volume data from calorimetric and dilatometric data is based on the principle of structural relaxation in silicate melts. The more general aspects of structural relaxation in silicate melts, their influence on diffusion, viscosity, heat capacity and density, have been discussed previously (e.g. Richet and Bottinga 1986; Dingwell 1990; Dingwell and Webb 1989, 1990). The theory of our procedure for obtaining relaxed-liquid molar expansivity data from a combination of scanning calorimetry and dilatometry has been presented in full by Webb et al. (1992).

The physical properties of a silicate melt depend upon the ambient temperature T and the configuration or structure of the melt. The configuration of silicate glasses quenched from liquids can be approximated to the equilibrium structure of the liquid at some fictive temperature, T_f. The temperature-derivatives of glass properties can be used to describe the temperature-derivative of the fictive temperature. To do this, the temperature-derivative of any property in the glass transition interval is normalized with respect

Table 4. Molar weight (g), glass and liquid densities (g cm^{-3}) and observed molar liquid volumes (cm^3 mole^{-1})

Temperature (°C)	21.3	1422	1522	1572	1622	1800	Molar weight
Densities							
Ab_{100}(B)	2.399	–	–	–	–	2.2594	262.225
An_{100}(B)	2.704	–	–	2.6033	2.5954	–	278.211
Di_{100}(B)	2.851	2.6340	2.6178	–	2.6010	–	216.553
Molar liquid volumes							
Ab_{100}(B)	111.181 (780 °C)	–	–	–	–	116.060	
An_{100}(B)	104.466 (920 °C)	–	–	106.869	107.194	–	
Di_{100}(B)	77.504 (810 °C)	82.215	82.723	–	83.258	–	

All volumes are $\pm 0.2\%$ at 1σ

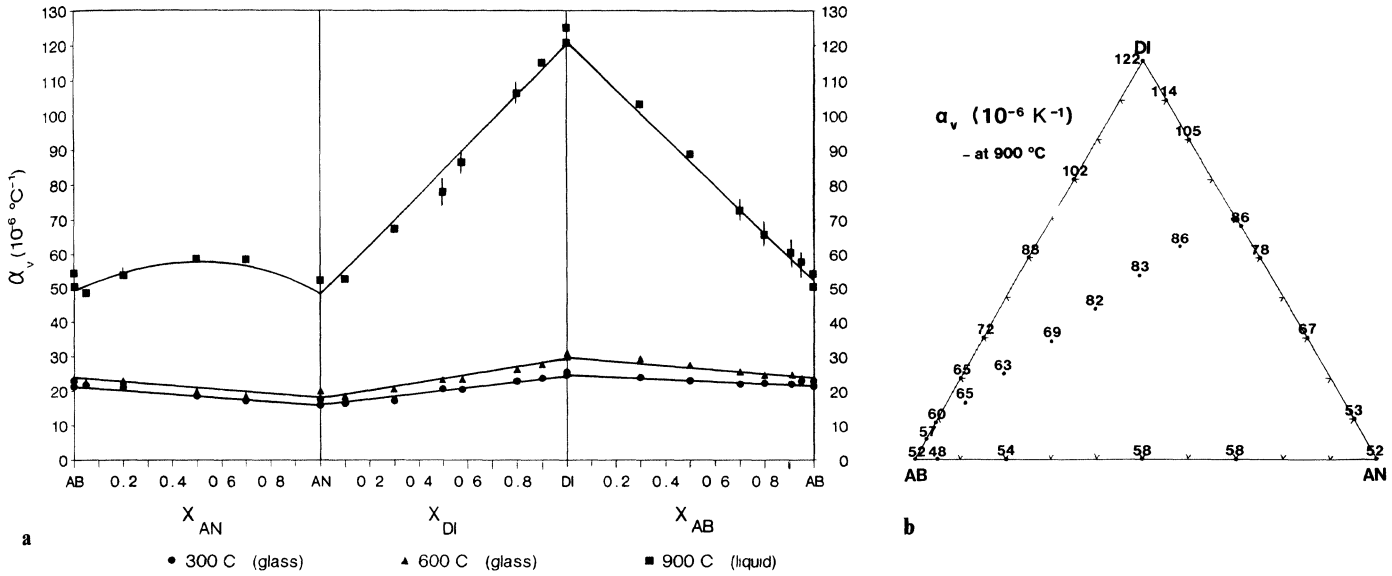

Fig. 3. **a** Coefficient of thermal expansion for the albite-anorthite-diopside binary systems for the glasses at 300 °C and 600 °C, and the melts at 900 °C. **b** Coefficient of thermal expansion for melts in the albite-anorthite-diopside ternary system at 900 °C

to the temperature-derivative of the liquid and glassy properties. The temperature-derivative of the fictive temperature T_f at a temperature T' is related to the temperature dependence of a macroscopic property Φ by;

$$\left.\frac{dT_f}{dT}\right|_{T'} = \frac{[(\partial\Phi/\partial T)-(\partial\Phi/\partial T)_g]|_{T'}}{[(\partial\Phi/\partial T)_e-(\partial\Phi/\partial T)_g]|_{T_f}} \quad (1)$$

where the subsripts e and g are for the liquid (equilibrium) and the glassy values of the property (Moynihan et al. 1976). In order to describe the physical properties of a melt in the glass transition region it is necessary to devise an algorithm for the temperature dependence of the fictive temperature.

In the present study, enthalpy H, and volume V take the place of the general property Φ in Eq. 1. Assuming the equivalence of volume and enthalpy relaxation behavior in the glass transition region (cf., Webb 1992), Eq. 1 can then be rewritten as (Webb et al. 1992; Knoche et al. 1992a);

$$\left.\frac{dT_f}{dT}\right|_{T'} = \frac{c_p(T')-c_{pg}(T')}{c_{pe}(T_f)-c_{pg}(T_f)} = \frac{\left.\frac{dV(T)}{dT}-\frac{dV_g(T)}{dT}\right|_{T'}}{\left.\frac{dV_e(T)}{dT}-\frac{dV_g(T)}{dT}\right|_{T_f}}. \quad (2)$$

In the above equation relating c_p and thermal expansivity dV/dT, the only unknown parameter is the thermal expansivity of the relaxed liquid at temperature T' above the glass transition temperature. The relaxed value of thermal expansivity now can be generated from the peak and extrapolated glassy values of the normalized heat capacity and thermal-expansion curves. The volume and coefficient of volume thermal expansion α_v $[1/V\cdot(dV/dT)]$ of the melt can also be calculated.

It should be emphasized that the above method only can be applied to calorimetric and dilatometric data obtained on the same sample using identical experimental conditions and thermal histories. It is only this internal consistency that permits the use of the assumption of the equivalence of the enthalpy and volume-relaxation behavior because small changes in composition or fictive temperature of the melt can strongly influence relaxation behavior.

Results

A typical set of calorimetric and dilatometric data is presented in Fig. 2a, b for the composition $Ab_{42}An_{21}Di_{37}$. The effect of viscous deformation in the liquid region of the dilatometric trace is clearly visible as a sharp drop in the expansivity above the peak value. The normalized comparison of relaxation in the dilatometric and calorimetric traces is illustrated in Fig. 2c. The thermal expansivity data for the glasses have been fitted to first order polynomials, with the resulting molar volume equations being presented in Table 3 and the coefficient of volume expansion for the glasses at 300 °C and 600 °C being illustrated in Fig. 3a. Expansivities of the supercooled liquids derived from the normalization procedure above, are presented in Table 5 together with the molar volumes at these temperatures. The coefficients of volume thermal expansion for the supercooled liquids at 900 °C are illustrated in Fig. 3a b.

For albite, anorthite and diopside compositions, superliquidus density and volume data are presented in Table 4. The molar volumes of these three samples at low and high temperatures together with the low-temperature thermal expansivity (dV/dT) have been combined and regressed against temperature using first and second order polynomials. The results of the least-squares regressions are reproduced in Table 6 (see also Fig. 4), together with the root-mean-squared deviations. The value of the supercooled dV/dT obtained from the dilatometry/calorimetry comparison is used to constrain the low-temperature slope of the curve fitted to the volume data. The inclusion of a temperature-derivative for the molar expansivity of albite and diopside liquid reduces the RMSD to within the error estimates of the volume data. In contrast, the anorthite volume data are described within error by a constant value of molar expansivity. The relaxed-liquid volume data from dilato-

Table 5. Measured values of dV/dT, α_v [$1/V \cdot (dV/dT)$] and molar volume for the supercooled liquids

	$\frac{dV}{dT}$ 10^{-4} cm^3 mole^{-1} °C^{-1}	α_v 10^{-6} °C^{-1}	V cm^3	T °C
Ab_{100}(B)	60.3±0.5	54.3±0.5	111.18±0.10	780
Ab_{100}(GM)	56.4±3.2	50.3±2.8	112.14±0.05	880
$Ab_{95}An_{05}$	53.8±1.7	48.5±1.5	110.91±0.09	880
$Ab_{80}An_{20}$	59.4±1.3	53.7±1.2	110.59±0.01	860
$Ab_{50}An_{50}$	62.6±1.3	58.4±1.2	107.09±0.02	860
$Ab_{30}An_{70}$	62.0±1.7	58.5±1.6	106.03±0.02	880
An_{100}(B)	54.4±2.1	52.0±2.0	104.47±0.01	920
An_{100}(GM)	54.6±1.2	52.4±1.2	104.20±0.05	920
$An_{90}Di_{10}$	53.5±0.8	52.4±0.8	102.01±0.05	900
$An_{70}Di_{30}$	65.0±1.7	67.4±1.8	96.44±0.05	860
$An_{50}Di_{50}$	70.5±3.9	78.0±4.3	90.44±0.02	830
$An_{42}Di_{58}$	76.6±2.8	86.3±3.1	88.80±0.03	820
$An_{20}Di_{80}$	87.8±2.3	106.2±2.8	82.63±0.04	810
$An_{10}Di_{90}$	93.0±1.2	115.3±1.5	80.64±0.03	810
Di_{100}(B)	96.9±1.9	125.1±2.6	77.50±0.22	810
Di_{100}(GM)	93.3±4.1	120.7±5.2	77.29±0.03	810
$Ab_{30}Di_{70}$	89.7±3.0	103.4±3.4	86.75±0.03	770
$Ab_{50}Di_{50}$	83.1±1.2	88.7±1.3	93.65±0.02	760
$Ab_{70}Di_{30}$	73.2±3.2	72.7±3.2	100.74±0.05	770
$Ab_{80}Di_{20}$	68.4±3.2	65.8±3.1	103.89±0.03	780
$Ab_{91}Di_{09}$	65.6±3.8	60.6±3.5	108.21±0.04	790
$AB_{95}Di_{05}$	63.1±2.7	57.8±2.6	109.25±0.25	810
$Ab_{82}An_{04}Di_{14}$	69.8±1.9	65.9±1.8	105.95±0.08	760
$Ab_{70}An_{09}Di_{21}$	67.2±1.1	65.1±1.1	103.08±0.02	770
$Ab_{70}An_{09}Di_{21}$ (+As)	64.8±1.3	62.8±1.3	103.15±0.01	770
$Ab_{56}An_{15}Di_{29}$	69.5±1.0	69.8±1.0	99.66±0.09	760
$Ab_{42}An_{21}Di_{37}$	80.0±0.7	82.8±0.8	96.59±0.02	770
$Ab_{28}An_{27}Di_{45}$	78.4±1.2	83.9±1.3	93.36±0.02	780
$Ab_{15}An_{32}Di_{53}$	78.6±1.2	86.9±1.4	90.41±0.02	800

Table 6. Molar liquid volumes $V(\text{cm}^3\ \text{mole}^{-1}) = a + b \times 10^{-3}\ T + c \times 10^{-6}\ T^2$ with T = temperature in °C

	a	b	c	$\sum(\text{residual})^2$
Ab_{100}(B)	105.73(0.05)	7.95(0.09)	−1.23(0.03)	0.0001
	107.43(0.09)	4.81(0.08)		0.0252
An_{100}(B)	100.36(1.52)	4.93(2.56)	−0.47(1.01)	0.0172
	101.07(0.05)	3.74(0.05)		0.0176
Di_{100}(B)	67.79(0.15)	14.47(0.28)	−3.05(0.12)	0.0016
	71.72(0.09)	7.23(0.09)		0.0988

metry/calorimetry and the superliquidus volume data for diopside, anorthite and albite are presented in Fig. 4 along with the polynomial fits to the data.

Discussion

The present room-temperature glass densities, 2.399 (B) and 2.381 (GM) ±0.003 g cm^{-3} for albite, 2.704 (B) and 2.714 (GM) ±0.003 g cm^{-3} for anorthite and 2.851 (B) and 2.863 (GM) ±0.003 g cm^{-3} for diopside, are within the range of those previously obtained for albite [2.363 g cm^{-3} (Day and Rindone 1962), 2.376 g cm^{-3} (Hayward 1976), and 2.385 g cm^{-3} (Kushiro 1978)]; anorthite [2.700 g cm^{-3} (Berman et al. 1942), 2.64 g cm^{-3} (Cukierman and Uhlmann 1973), 2.701 g cm^{-3} (Arndt and Häberle 1973), 2.66 g cm^{-3} (Seifert et al. 1982), and 2.704 g cm^{-3} (Taniguchi 1989)]; and for diopside [2.846 g cm^{-3} (Berman et al. 1942); 2.870 g cm^{-3} (Taniguchi 1989)]. The densities of glasses are dependent on thermal history and this, combined with slight compositional variations precludes a closer comparison of the glass data.

The superliquidus density of albite liquid is the first determination of liquid density for this composition. Stein et al. (1986) have determined the densities of peralkaline liquids in the $Na_2O-Al_2O_3-SiO_2$ system and provide partial molar volumes for Na_2O, Al_2O_3 and SiO_2 in the temperature range of 1,100 °C to 1,550 °C. These partial molar volumes, extrapolated in composition to albite, reproduce our direct determinations within the uncertainties involved. The present determination of

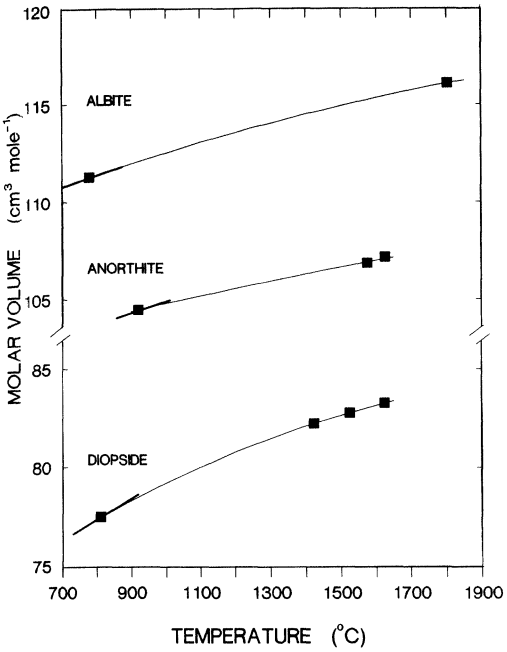

Fig. 4. Relaxed-liquid volume data from dilatometry and densitometry for albite, anorthite and diopside. The *thicker lines* at low temperature indicate the measured low-temperature thermal expansivity (dV/dT)

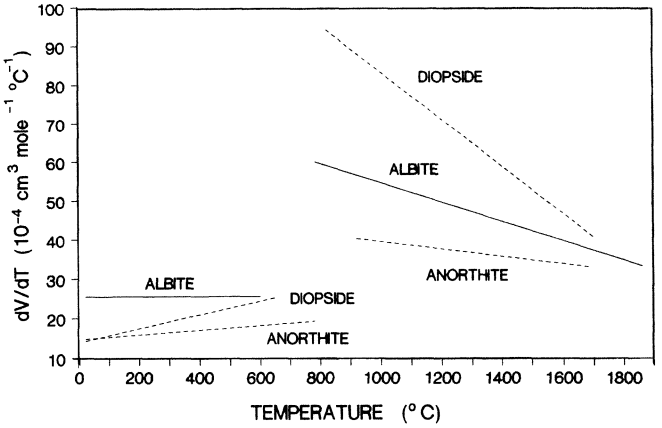

Fig. 5. dV/dT for albite; anorthite; and diopside from room temperature up to superliquidus temperatures

the glass transition temperature of albite is also of interest. Although the two glasses investigated have a composition difference of only 1 wt% Na_2O, there is a 100 °C difference in glass transition temperature – determined using the same method and the same definition of the glass transition temperature. In the case of the anorthite and diopside compositions, no variation in glass transition temperature is observed. Despite this variation in the glass transition temperature of the two albite compositions, the thermal expansivities for the two melts are, within error, the same. Richet and Bottinga (1984b) in their calorimetric study of albite glasses also found the glass transition temperature to be sensitive to composition variations, but the heat capacity of the melts remained unaffected by slight variations in composition.

The superliquidus density of diopside liquid has been investigated by Licko and Danek (1982) using the falling sphere method and by Lange and Carmichael (1987) and Taniguchi (1989) using the double Pt bob method. As noted by Knoche et al. (1992a) the results of Lange and Carmichael (1987) and Taniguchi (1989) agree well with our diopside density data while those of Licko and Danek (1982) are 1% lower. The density of melts on the anorthite-diopside join has been investigated by Taniguchi (1989). Our anorthite density at 1,580 °C (2.6007 ± 0.0121 g cm^{-2}) is higher than that determined by Taniguchi (1989) (2.538 g cm^{-3}) and that calculated from the scheme of Lange and Carmichael (1990) (2.5649 g cm^{-3}). The reasons for this discrepancy for anorthite melt are not clear.

The thermal expansivity of supercooled liquids in the anorthite-diopside system has been investigated previously using dilatometric techniques. Taniguchi (1989) used the transient peak values of thermal expansivity (the maximum in the dV/dT curve) for the supercooled liquid. This resulted in thermal expansivities that were consistently too high to reproduce the high-temperature volumes of this liquids. His Fig. 5 illustrates the contrast between the coefficient of thermal expansion (240×10^6 °C^{-1}) determined at the maximum in the dV/dT curve and the coefficient of thermal expansion (125×10^6 °C^{-1}) obtained from a polynomial fit to high- and low-temperature liquid density data, for diopside. A similar procedure was used by Arndt and Häberle (1973) to determine the thermal expansion of anorthite liquid in the vicinity of the glass transition temperature.

In the present study our measured thermal expansivities near T_g are consistent with the values obtained from our volume fits as seen in Table 5 and 6. Our measured and fitted (2nd order polynomial) values of the coefficient of thermal expansion for diopside at 810 °C are 125×10^{-6} °C^{-1} and 123×10^{-6} °C^{-1} respectively. This agreement removes the discrepancy posed by the Taniguchi (1989) data and improves considerably confidence in the prediction of low-temperature melt densities.

An inspection of Fig. 4 indicates that extrapolation of diopside volume data either up or down temperature from the segments of the volume curve covered by either method, will result in serious overestimates of liquid volume. The extrapolation of high-temperature volumes and expansivity to low temperature yields a 3% error. This discrepancy lies outside the accuracy of multicomponent calculation schemes presently available (e.g., Lange and Carmichael 1990). Clearly, a much more complete investigation of the temperature-dependence of liquid expansivity is required to incorporate this correction in such schemes.

Conclusion

The method developed by Webb et al. (1992) for extrapolation of liquid expansivity based on the concept of the equivalence of volume and enthalpy relaxation has been demonstrated to yield volume and thermal expansivity

data consistent with the available high-temperature density data for silicate melts. The combination of corrected low-temperature density/expansivity data and high-temperature density/expansivity data allows us to interpolate melt density through the experimentally inaccessible temperature interval below the liquidus that is so important for igneous petrogenesis. The gap in data as a function of temperature observed in Fig. 1 is essentially removed with the use of the present technique, as seen in Fig. 5.

The resulting improvement in the precision of thermal expansivity data allows the detection of temperature-dependent thermal expansion for some melt compositions. In principle the determination of liquid expansivities at low temperature allows the temperature correction of liquid volume data obtained at varying glass transition temperatures for varying composition. Thus the partial molar volumes of melt components that are experimentally inaccessible at high temperature can be derived at lower temperatures. One example of this is the case of volatile elements (e.g., P_2O_5, F, B_2O_3) in high viscosity melts such as haplogranites, determined at magmatic temperatures (cf., Knoche et al. 1992b).

Acknowledgements. We thank Kurt Klasinski for software development and Detlef Krauße for microprobe analyses. The calorimetry was supported by a Leibniz Prize to F. Seifert.

References

Arndt J, Häberle F (1973) Thermal expansion and glass transition temperatures of synthetic glasses of plagioclase-like compositions. Contrib Mineral Petrol 39:175–183

Berman H, Daly RA, Spicer HC (1942) Density at room temperature and 1 atmosphere. In: Birch F, et al. (eds) Handbook of Physical Constants Geol Soc Am, No 36, pp 7–26

Bottinga Y, Weill DF (1970) Density of liquid silicate systems calculated from partial molar volumes of oxide components. Am J Sci 269:169–182

Bottinga Y, Weill D, Richet P (1983) Calculation of the density and thermal expansion coefficient of silicate liquids. Bull Mineral 104:129–138

Bowen NL (1915) The crystallization of haplobasaltic, haplodioritic and related magmas. Am J Sci 40:161–185

Cukierman M, Uhlmann DR (1973) Viscosity of liquid anorthite. J Geophys Res 78:4920–4923

Day DE, Rindone GE (1962) Properties of soda aluminosilicate glasses: 1, refractive index, density, molar refractivity, and infrared absorption spectra. J Am Ceram Soc 45:489–496

Dingwell DB (1990) Effects of structural relaxation on cationic tracer diffusion in silicate melts. Chem Geol 82:209–216

Dingwell DB (1991) The density of TiO_2 liquid. J Am Ceram Soc 74:2718–2719

Dingwell DB, Webb SL (1989) Structural relaxation in silicate melts and non-Newtonian melt rheology in geologic processes. Phys Chem Miner 16:508–516

Dingwell DB, Webb SL (1990) Relaxation in silicate melts. Eur J Mineral 2:427–449

Dingwell DB, Brearley M, Dickinson Jr JE (1988) Melt densities in the $Na_2O-FeO-Fe_2O_3-SiO_2$ system and the partial molar volume of tetrahedrally coordinated ferric iron in silicate melts. Geochim Cosmochim Acta 52:2467–2475

Hayward PJ (1976) The mixed alkali effect in aluminosilicate glasses, part 1: the join $SiO_2-(Na,K)AlSi_3O_8$. Phys Chem Glasses 17:54–61

Janz GJ (1980) Molten salts data as reference data for density, surface tension, viscosity and electrical conductance. J Phys Chem Ref Data 9:791–829

Knoche R (1990) Untersuchungen der Glastransformationstemperatur im System Albit-Anorthit-Diopsid mit Hilfe der DTA. Diplomarbeit, Georg-August-Universität, Göttingen

Knoche R, Dingwell DB, Webb SL (1992a) Temperature-dependent thermal expansivities of silicate melts: the system anorthite-diopside. Geochim Cosmochim Acta 56:689–699

Knoche R, Webb SL, Dingwell DB (1992b) A partial molar volume for B_2O_3 in haplogranitic melt. Can Mineral (accepted)

Kushiro I (1973) The system diopside-anorthite-albite: determination of compositions of coexisting phases. Carnegie Inst Washington Yearb 72:502–507

Kushiro I (1978) Viscosity and structural changes of albite ($NaAlSi_3O_8$) melt at high pressures. Earth Planet Sci Lett 41:87–90

Lange RA, Carmichael ISE (1987) Densities of $K_2O-Na_2O-CaO-MgO-FeO-Fe_2O_3-Al_2O_3-TiO_2-SiO_2$ liquids: new measurements and derived partial molar properties. Geochim Cosmochim Acta 51:2931–2946

Lange RA, Carmichael ISE (1990) Thermodynamic properties of silicate liquids with emphasis on density, thermal expansion and compressibility. In: Nicholls J, Russel JK (eds) Modern Methods of Igneous Petrology. Mineral Soc Am, Washington, pp 25–64

Licko T, Danek V (1982) Densities of melts in the system $CaSiO_3-CaMgSi_2O_6-Ca_2MgSi_2O_7$. Phys Chem Glasses 23:67–71

Moynihan CT, Easteal AJ, DeBolt MA, Tucker J (1976) Dependence of fictive temperature of glass on cooling rate. J Am Ceram Soc 59:12–16

Navrotsky A, Hon R, Weill DF, Henry DJ (1980) Thermochemistry of glasses and liquids in the system $CaMgSi_2O_6-CaAl_2Si_2O_8-NaAlSi_3O_8$, $SiO_2-CaAl_2Si_2O_8-NaAlSi_3O_8$ and $SiO_2-Al_2O_3-CaO-Na_2O$. Geochim Cosmochim Acta 44:1409–1423

Navrotsky A, Ziegler D, Oestrike R, Maniar P (1989) Calorimetry of silicate melts at 1773K: measurement of enthalpies of fusion and of mixing in the systems diopside-anorthite-albite and anorthite-forsterite. Contrib Mineral Petrol 101:122–130

Osborn EF, Tait DB (1952) The system diopside-forsterite-anorthite. Am J Sci Bowen Volume: 413–433

Richet P, Bottinga Y (1984a) Anorthite, andesine, wollastonite, diopside, cordierite and pyrope: thermodynamics of melting, glass transition, and properties of the amorphous phase. Earth Planet Sci Lett 67:415–432

Richet P, Bottinga Y (1984b) Glass transitions and thermodynamic properties of amorphous SiO_2, $NaAlSi_nO_{2n+2}$ and $KAlSi_3O_8$. Geochim Cosmochim Acta 48:453–470

Richet P, Bottinga Y (1986) Thermophysical properties of silicate glasses and liquids. Rev Geophys 24:1–25

Rigden S, Ahrens TJ, Stolper EM (1988) Shock compression of molten silicate: results for a model basaltic composition. J Geophys Res 93:367–382

Rigden S, Ahrens TJ, Stolper EM (1989) High-pressure equation of state of molten anorthite and diopside. J Geophys Res 94:9508–9522

Rivers ML, Carmichael ISE (1987) Ultrasonic studies of silicate melts. J Geophys Res 92:9247–9270

Robie RA, Hemmingway BS, Fisher JR (1979) Thermodynamic properties of minerals and related substances at 298.15 K and 1 bar (10^5 Pascals) pressure and at higher temperatures. USGS Printing Office, Washington

Scarfe CM, Cronin DJ (1986) Viscosity-temperature relationships of melts at 1 atm in the system diopside-albite. Am Mineral 74:767–771

Scarfe CM, Cronin DJ, Wenzel JT, Kaufmann DA (1983) Viscosity-temperature relationships at 1 atm in the system diopside-anorthite. Am Mineral 68:1083–1088

Schairer JF, Yoder Jr HS (1960) The nature of residual liquids from crystallization, with data on the system nepheline-diopside-silica. Am J Sci 258A:273–283

Seifert FA, Mysen BO, Virgo D (1982) Three-dimensional network structure of quenched melts (glasses) in the system $SiO_2-NaAlO_2$, $SiO_2-CaAl_2O_4$ and $SiO_2-MgAl_2O_4$. Am J Sci 67:696–717

Stebbins JF, Weill DE, Carmichael ISE, Moret LK (1982) High temperature heat contents and heat capacities of liquids and glasses in the system $NaAlSi_3O_8-CaAl_2Si_2O_8$. Contrib Mineral Petrol 80:276–284

Stebbins JF, Carmichael ISE, Weill DE (1983) The high temperature liquid and glass heat contents and the heats of fusion of diopside, albite, sanidine and nepheline. Am Mineral 68:717–730

Stein DJ, Stebbins JF, Carmichael ISE (1986) Density of molten sodium aluminosilicates. J Am Ceram Soc 69:396–399

Taniguchi H (1989) Densities of melts in the system $CaMgSi_2O_6-CaAl_2Si_2O_8$ at low and high pressures, and their structural significance. Contrib Mineral Petrol 103:325–334

Tauber P (1987) Viskositätsuntersuchungen im Modellsystem Anorthit-Albit-Diopsid. Dissertation. Eberhard-Karls-Universität, Tübingen

Tauber P, Arndt J (1987) The relationship between viscosity and temperature in the system anorthite-diopside. Chem Geol 62:71–81

Webb SL (1992) Shear, enthalpy, volume and structural relaxation in silicate melts. Chem Geol (accepted)

Webb SL, Knoche R, Dingwell DB (1992) Determination of silicate liquid thermal expansivity using dilatometry and calorimetry. Eur J Mineral 4:95–104

Weill DF, Hon R, Navrotsky A (1980) The igneous system $CaMgSi_2O_6-CaAl_2Si_2O_8-NaAlSi_3O_8$: variations on a classic theme by Bowen. In: Hargraves RB (ed) Physics of Magmatic Processes. Princeton University Press, Princeton, pp 49–92

Editorial responsibility: W. Schreyer